

Effects of Sr²⁺ on the properties of layered perovskite structured Ba_{1-x}Sr_xTi₄O₉ ceramics

S. Uddin^a, A. Ali^{b,c}, A. Zaman^{b,*}, H. Alrobei^d, A. H. Alghtani^e, V. Tirth^{f,g},
A. Algahtani^{f,g}, F. Ullah^c

^aDepartment of Physics, Government College Hayatabad, Peshawar 25000, Pakistan

^bDepartment of Physics, Riphah International University, Islamabad 44000, Pakistan

^cDepartment of Physics, Government Postgraduate College, Nowshera 24100, Pakistan

^dDepartment of Mechanical Engineering, College of Engineering, Prince Sattam Bin Abdulaziz University, Alkharj 11942, Saudi Arabia

^eDepartment of Mechanical Engineering, College of Engineering, Taif University, P.O. Box 11099, Taif 21944, Kingdom of Saudi Arabia.

^fMechanical Engineering Department, College of Engineering, King Khalid University, Abha 61421, Asir, Kingdom of Saudi Arabia

^gResearch Center for Advanced Materials Science (RCAMS), King Khalid University Guraiger, Abha-61413, Asir, P.O. Box No. 9004, Kingdom of Saudi Arabia.

The Phase, microstructural and dielectric properties of Ba_{1-x}Sr_xTi₄O₉ (0 ≤ x ≤ 0.8) ceramics were investigated. The XRD analysis revealed the formation of orthorhombic structured (Pnmm) BaTi₄O₉ phase. The XRD peaks were observed to shift towards the lower 2θ values with increasing Sr²⁺ contents which may be attributed to the substitution of relatively larger cation of Sr²⁺ (R_{Sr} = 1.61 Å) for Ba²⁺ (R_{Ba} = 1.44 Å) in BaTi₄O₉. The dielectric constant (ε_r) increased with Sr²⁺ substitution from 22 to 122 at 1MHz. The maximum value of the dielectric loss was observed 0.11922 for x = 0.8 at 1 MHz.

(Received April 3, 2022; Accepted July 19, 2022)

Keywords: Perovskites, Dielectric resonator, Microwave dielectrics, Mixed oxides

1. Introduction

Dielectric materials are used extensively as piezoelectric transducers and actuators, as ferroelectric memory and energy storage devices or as dielectric antenna and filter in wireless telecommunication devices [1-3]. The Electronic Industries Alliance (EIA) in USA classifies ceramic dielectrics into different categories depending on their dielectric constant, also known as relative permittivity (ε_r) [4]. This property of a dielectric material determines the amount of energy that a capacitor can store compared to vacuum. Dielectrics are further divided into three sub-classes depending on their thermal and dielectric characteristics. We restrict our discussions only to class-1 dielectrics.

Class-1 dielectrics are commonly used in capacitors exhibited temperature stable performance, low acoustic noise and low dielectric loss. COG is one of the types of capacitors frequently used in filter circuits and high-frequency circuits. Other applications of class-1 capacitors are DC blocking, tuning, transient voltage suppression, energy storage, critical timing, decoupling, data acquisition filters and PLL low pass filter. Class-1 dielectrics usually exhibited lower dissipation factor (15%), medium dielectric constant (15–500) and negligible aging effect

* Corresponding author: zaman.abid87@gmail.com
<https://doi.org/10.15251/DJNB.2022.173.793>

[5]. Class-1 dielectric mainly includes paraelectrics, MgTiO_3 , MgNb_2O_6 , BaTi_4O_9 and their isostructure compounds. Among oxides compounds used as class-1 dielectrics, BaTi_4O_9 is one of the dielectric materials reported first by Rase and Roy [6]. The dielectric material components were used in wireless equipment for transmitting and receiving of electromagnetic signals are termed as dielectric resonators (DRs) which is reported by Richtmyer in 1939 for first time and A. Ali et.al [7-10]. The optimum commercial properties of a dielectric resonator includes high relative permittivity (ϵ_r) for miniaturization, high quality factor ($Q \times f$) for noise reduction and near to zero temperature coefficient of resonant frequency (τ_f) required for thermal stability [11]. A typical dielectrically loaded antenna requires; ϵ_r from 20 to 85, $(Q \times f) \geq 10000$ GHz and $\tau_f \sim \pm 2$ ppm/ $^\circ\text{C}$ [12]. The dielectric and structural properties of BaTi_4O_9 with different additives have been investigated at various frequencies. Several studies were carried out to improve the dielectric properties of BaTi_4O_9 ceramics by different substitutions for Ba^{2+} and Ti^{4+} [13-19].

In the present work the effects of Sr^{2+} doping on Phase, microstructure and dielectric properties of BaTi_4O_9 were investigated.

2. Experimental

Solid solutions of $(\text{Ba}_{1-x}\text{Sr}_x)\text{Ti}_4\text{O}_9$, ($0 \leq x \leq 0.8$) were obtained via conventional solid state route. Research grade, BaCO_3 , SrCO_3 and TiO_2 were mixed according to the stoichiometric ratios. The powder was crushed by a horizontal ball mill for 12 h in a polymer jar with zirconia balls of 5 mm diameter as grinding media and distilled water for lubrication purpose. After milling the slurry was dried in oven at 90°C for 8h in air. The dried reactants powder was calcined in an alumina crucible at 1000°C for 2.5 h in air with $5^\circ\text{C}/\text{min}$ heating and cooling rates. After calcination the product powder was pulverized manually with a pistol and mortar to avoid agglomeration. The fine powders were pressed with a uniaxial presser in disc shapes of about 4 mm thick and 10 mm in diameter under 100 MPa pressure. The green discs were sintered at 1300°C for 2 h in air with $5^\circ\text{C}/\text{min}$ of heating and cooling rates.

The phase and microstructural analyses were carried out by using X-Ray diffractometer (XRD) (JDX-3532, JEOL, Japan) with Cu , $\text{K}\alpha$ radiation ($\lambda = 0.154$ nm) and scanning electron microscope (SEM) (JSM-5910, JEOL Japan) respectively. The apparent densities of the sintered ceramic pellets were measured by densitometer (MD 300s) using the Archimedes principle. The microwave dielectric properties of the fabricated ceramic pellets were measured by LCR meter (Agilent 4287A).

3. Results and discussions

3.1. Phase analyses

The XRD patterns of $\text{Ba}_{1-x}\text{Sr}_x\text{Ti}_4\text{O}_9$ ($0 \leq x \leq 0.8$) calcined powders are shown in the Fig. 1. XRD analysis revealed the formation of the base composition barium tetratitanate, BaTi_4O_9 (Orthorhombic, Pnmm) matched with ICDD, PDF card # 34-70. It is suggested that Sr^{2+} are incorporated in the lattice of the base composition to replace Ba^{2+} ions. The XRD peaks were observed to shift towards the lower 2θ values with increasing Sr^{2+} contents in $(\text{Ba}_{1-x}\text{Sr}_x)\text{Ti}_4\text{O}_9$ which may be attributed to the substitution of relatively larger cation of Sr^{2+} ($R_{\text{Sr}} = 1.61$ Å) for Ba^{2+} ($R_{\text{Ba}} = 1.44$ Å) following the Brags diffraction law ($2d\sin\theta = m\lambda$) [20]. A peak at 32.4° emerges with increase in content x which is attributed to the transformation of the structure from orthorhombic at $x = 0$ to tetragonal at $x = 0.2, 0.4$ and then to cubic at $x = 0.6, 0.8$. The peak at 31.5° disappear completely at $x = 0.8$. The variation in lattice parameters with increasing Sr^{2+} content is attributed to the phase transition from orthorhombic to tetragonal and then to cubic structure as listed in Table 1.

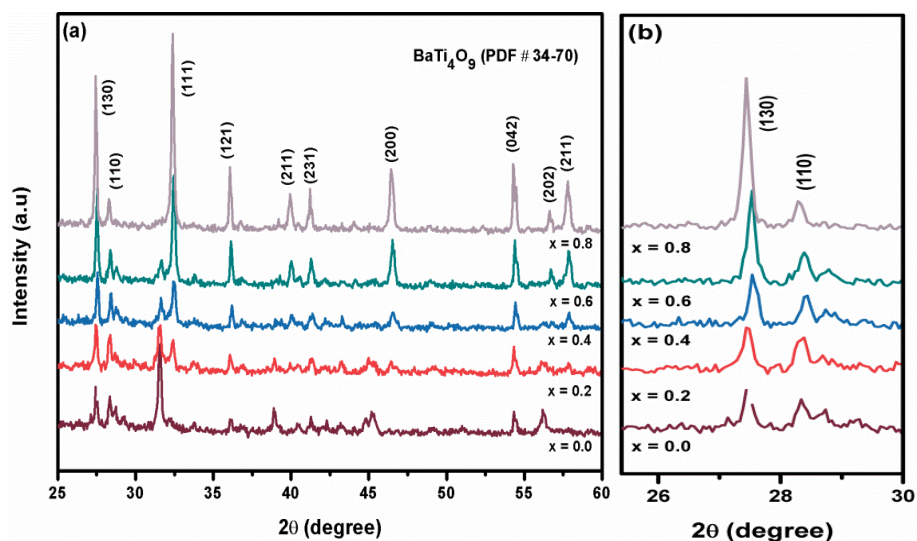


Fig. 1. (a) XRD patterns of $(\text{Ba}_{1-x}\text{Sr}_x)\text{Ti}_4\text{O}_9$, $0 \leq x \leq 0.8$ powders calcined at 1000°C in air (b) Shifting of (130) peak to lower 2θ values with increasing Sr^{2+} content.

Table 1. Structural data of $\text{Ba}_{1-x}\text{Sr}_x\text{Ti}_4\text{O}_9$ ($0 \leq x \leq 0.8$) obtained from XRD analysis.

x	Structure	Space group	a (Å)	b (Å)	c (Å)
0	Orthorhombic	Pnmm	6.2940	14.5324	3.7972
0.2	Tetragonal	I4/m	10.1434	10.1434	2.96795
0.4	Tetragonal	I4/m	10.1434	10.1434	2.96795
0.6	Cubic	Pm3m	3.8980	3.8980	3.8980
0.8	Cubic	Pm3m	3.907	3.907	3.907

3.2. Microstructural analysis

The SEM images of $\text{Ba}_{1-x}\text{Sr}_x\text{Ti}_4\text{O}_9$ ($0 \leq x \leq 0.8$) ceramics sintered at 1300°C in air for 2 h, polished and thermally etched are shown in Fig.2.

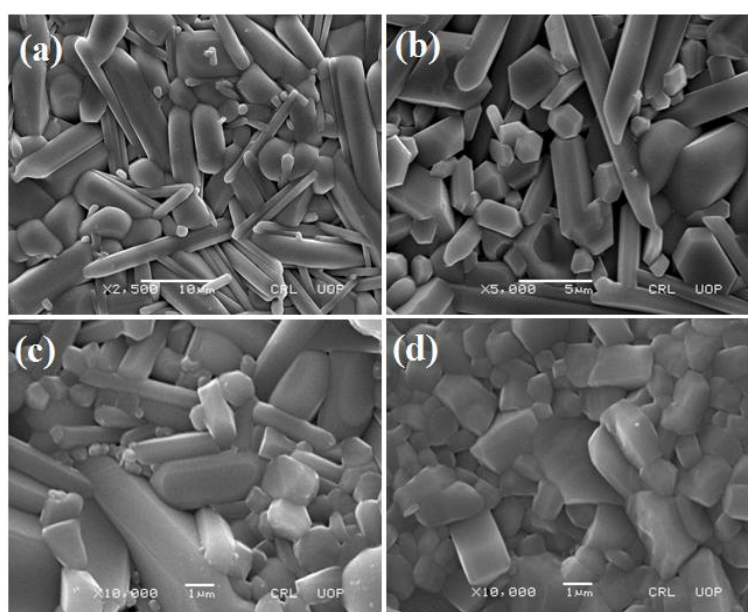


Fig. 2. SEM images of $\text{Ba}_{1-x}\text{Sr}_x\text{Ti}_4\text{O}_9$ ($0 \leq x \leq 0.8$) ceramics polished, thermally etched and sintered at 1300°C for 2 h in air; (a) $x = 0$, (b) $x = 0.2$, (c) $x = 0.6$, (d) $x = 0.8$; indicating a decrease in grain size and change in grain morphologies with increase in x .

The SEM images indicated dense microstructure with no obvious pores and grains exhibited elongated plate-like morphologies for the Base composition $x=0$, consistent with previous reports for the orthorhombic structured BaTi_4O_9 [21, 22]. The grains morphologies were observed to change from elongated shapes to rectangular shapes with increase in the Sr^{2+} contents. The grain size for $x=0$ is about $10 \times 1 \mu\text{m}^2$ and decreases with increase in Sr^{2+} content. The variation of the relative densities (ρ_r) with increasing the Sr^{2+} content is shown in the Fig.3 (a). The maximum theoretical density achieved is 5.84 g/cm^3 as listed in table 2. The increase in density affects the dielectric constant as shown in Fig. 3.3 [23].

3.3. Dielectric properties

The Variation in dielectric constant (ϵ_r) and dielectric loss ($\tan \delta$) with frequency (f) of applied electric field for various Sr^{2+} content is shown in Fig. 3. The dielectric constant decreased accompanied with increase in dielectric loss monotonically with increasing frequency of the electric field. The orientation polarization decreases with increasing frequency and resulted a decrease in ϵ_r which may be attributed to time lagging between flipping dipoles and applied electric field [24]. Variation in dielectric constant and dielectric loss with frequency for various Sr^{2+} content in $\text{Ba}_{1-x}\text{Sr}_x\text{Ti}_4\text{O}_9$ ($0 \leq x \leq 0.8$) ceramics at 1 MHz are listed in Table 2. For Microwave dielectric applications class-1 dielectrics are characterized by the product $Q \times f$ (f measured in GHz) which is assumed to be constant [5]. Here $Q = 1 / \tan \delta$ is quality factor which is frequency dependent dimensionless quantity [12, 19]. The theoretical justification for GHz measurement is that in the case of an ionic solid the optical mode of the lattice vibration resonates at frequencies in the region around 10^{13} Hz. In the frequency range from approximately 10^9 – 10^{11} Hz dielectric dispersion theory shows the contribution to polarization from the ionic displacement to be nearly constant and the losses to rise with frequency. However, the relationship is at best a rough guide and there is no alternative to the measurement if reliable loss data at a particular frequency are obtained [25].

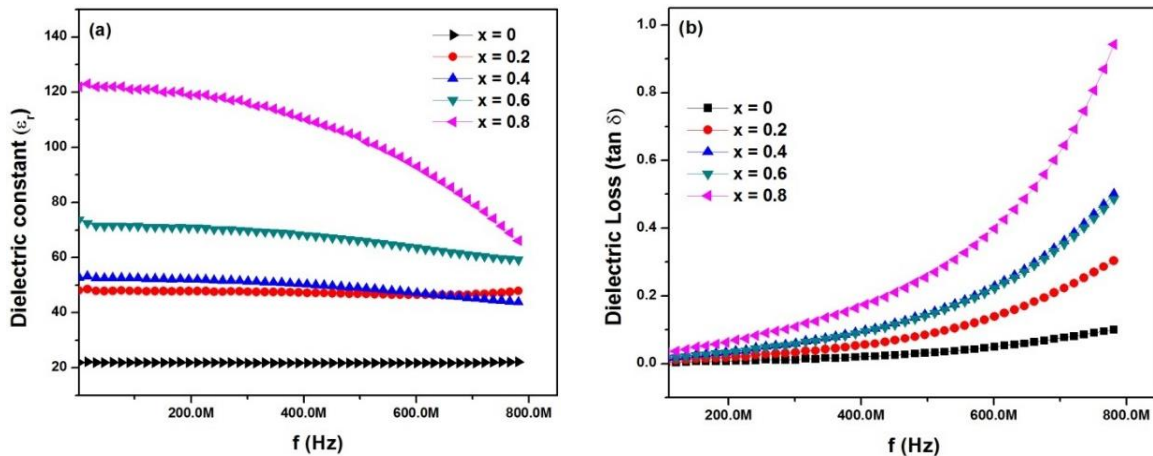


Fig. 3. (a) Variation in dielectric constant (ϵ_r) with frequency (f) (b) Variation in dielectric loss ($\tan \delta$) with frequency (f) for various Sr^{2+} content in $\text{Ba}_{1-x}\text{Sr}_x\text{Ti}_4\text{O}_9$ ($0 \leq x \leq 0.8$) ceramics.

Table 2. Dielectric properties of $\text{Ba}_{1-x}\text{Sr}_x\text{Ti}_4\text{O}_9$ ($0 \leq x \leq 0.8$) sintered ceramic samples at 1 MHz frequency.

X	S.T (°C)	ρ_a (g/cm ³)	ρ_t (g/cm ³)	ρ_r (%)	ϵ_r	$\tan \delta$
0	1300 °C/2h	4.26	4.82	88.38	21.9	0.01474
0.2	1300 °C/2h	4.40	5.840	75.37	48.0	0.03759
0.4	1300 °C/2h	4.40	4.940	89.07	52.8	0.06458
0.6	1300 °C/2h	4.07	5.140	79.12	73.7	0.06645
0.8	1300 °C/2h	3.99	4.400	90.68	122.0	0.11922

S.T= Sintering temperature, ρ_a = apparent density, ρ_t =theoretical density, ρ_r =relative density

5. Conclusion

Ceramic samples of $\text{Ba}_{1-x}\text{Sr}_x\text{Ti}_4\text{O}_9$ ($0 \leq x \leq 0.8$) were synthesized through mixed oxide route. The phase analysis revealed the formation of orthorhombic structured, BaTi_4O_9 . The SEM images indicated dense microstructure with no obvious pores and grains exhibited elongated plate-like morphologies for the base composition. The dielectric constant (ϵ_r) varies from 22 for $x = 0$ to 122 for $x = 0.8$ at 1 MHz. The fabricated compositions may be promising materials for dielectric applications.

Acknowledgments

The research was supported by the Taif University Researchers Supporting Project number (TURSP-2020/349), Taif University, Taif, Kingdom of Saudi Arabia. The authors extend their appreciation to the Deanship of Scientific Research at King Khalid University Abha 61421, Asir, Kingdom of Saudi Arabia for funding this work through the Large Groups Project under grant number RGP.2/225/43.

References

- [1] Reaney, I. M., & Iddles, D. (2006), *Journal of the American Ceramic Society*, 89(7), 2063-2072; <https://doi.org/10.1111/j.1551-2916.2006.01025.x>
- [2] Hao, X. (2013), *Journal of Advanced Dielectrics*, 3(01), 1330001; <https://doi.org/10.1142/S2010135X13300016>
- [3]. Jo, W., & Rödel, J. (2011), *Applied Physics Letters*, 99(4), 042901; <https://doi.org/10.1063/1.3615675>
- [4] Kao, K. C. (2004). *Dielectric phenomena in solids* Elsevier Academic Press.
- [5] Moulson, A. J., & Herbert, J. M. (2003). *Electroceramics: materials, properties, applications*. John Wiley & Sons; <https://doi.org/10.1002/0470867965>
- [6] Rase, D. E., & Roy, R. (1955), *Journal of the American Ceramic Society*, 38(3), 102-113; <https://doi.org/10.1111/j.1151-2916.1955.tb14585.x>
- [7] Richtmyer, R. D. (1939), *Journal of Applied Physics*, 10(6), 391-398; <https://doi.org/10.1063/1.1707320>
- [8] A. Ali, S. Uddin, A. Zaman, A. Ahmad, & Z. Iqbal, *Advances in Applied Ceramics*, 119(8), 482-486 (2020); <https://doi.org/10.1080/17436753.2020.1840267>
- [9] M. Abbas, R. Ullah, K. Ullah, F. Sultana et al., *Ceramics International*, 47(21), 30129-30136 (2021); <https://doi.org/10.1016/j.ceramint.2021.07.191>
- [10] A. Ali, S. Uddin, Z. Iqbal et al., *Journal of Materials Research and Technology*, 11, 1828-1833 (2021); <https://doi.org/10.1016/j.jmrt.2021.01.126>
- [11]. A. Zaman, S. Uddin, N. Mehboob & A. Ali, *Physica Scripta*, 96(2), 025701 (2020); <https://doi.org/10.1088/1402-4896/abce74>
- [12] R. Muhammad, Y. Iqbal, I.M. Reaney, J. Alloys. *Compd.* 646 (2015) 368-371; <https://doi.org/10.1016/j.jallcom.2015.06.038>
- [13] O'Bryan Jr, H. M., Thomson Jr, J., & Plourde, J. K. (1974), *Journal of the American Ceramic Society*, 57(10), 450-453; <https://doi.org/10.1111/j.1151-2916.1974.tb11380.x>
- [14]. Mhaisalkar, S. G., Readey, D. W., Akbar, S. A., Dutta, P. K., Sumner, M. J., & Rokhlin, R. (1991), *Journal of Solid State Chemistry*, 95(2), 275-282; [https://doi.org/10.1016/0022-4596\(91\)90106-R](https://doi.org/10.1016/0022-4596(91)90106-R)
- [15] Nishigaki, S., Yano, S., Kato, H., Hirai, T., & Nonomura, T. (1988), *Journal of the American Ceramic Society*, 71(1), C-11; <https://doi.org/10.1111/j.1151-2916.1988.tb05769.x>
- [16] Ern, V., & Newnham, R. E. (1961), *Journal of the American Ceramic Society*, 44(4), 199-

- 199; <https://doi.org/10.1111/j.1151-2916.1961.tb13746.x>
- [17] Kolar, D., Gaberscek, S., Volavsek, B., Parker, H. S., & Roth, R. S. (1981), *Journal of Solid State Chemistry*, 38(2), 158-164; [https://doi.org/10.1016/0022-4596\(81\)90030-X](https://doi.org/10.1016/0022-4596(81)90030-X)
- [18] Cernea, M. (2007), *Journal of optoelectronics and advanced materials*, 9(12), 3790-3794.
- [19] Choi, Y. J., Park, J. H., Ko, W. J., Park, J. H., Nahm, S., & Park, J. G. (2005), *Journal of electroceramics*, 14(2), 157-162; <https://doi.org/10.1007/s10832-005-0880-8>
- [20] Shannon, R. D. (1976), *Acta Cryst. A*, 32, 751-767.
- [21] Ma, H., Zhang, W., Kong, X., Uemura, S., Kusunose, T., & Feng, Q. (2019), *Journal of Alloys and Compounds*, 777, 335-343; <https://doi.org/10.1016/j.jallcom.2018.10.339>
- [22] Luo, T., He, L., Yang, H., & Yu, H. (2019), *International Journal of Applied Ceramic Technology*, 16(1), 146-151; <https://doi.org/10.1111/ijac.13073>
- [23] Muhammad, R., Iqbal, Y., & Reaney, I. M. (2015), *Journal of Alloys and Compounds*, 646, 368-371; <https://doi.org/10.1016/j.jallcom.2015.06.038>
- [24] Sebastian, M. T., Uvic, R., & Jantunen, H. (2015), *International Materials Reviews*, 60(7), 392-412; <https://doi.org/10.1179/1743280415Y.0000000007>
- [25] Sebastian, M. T. (2010). *Dielectric materials for wireless communication*. Elsevier.